Original Article

Noninvasive Monitoring of Diabetes-Induced Cutaneous Nerve Fiber Loss and Hypoalgesia in *thy1*-YFP Transgenic Mice

Yuk Shan Chen,[1] Stephen S.M. Chung,[2] and Sookja K. Chung[1]

Progressive loss of pain perception and cutaneous nerve fibers are frequently observed in diabetic patients. We evaluated the feasibility of using *thy1*-YFP mice that express the yellowish-green fluorescent protein (YFP) in all of their sensory/motor neurons for noninvasive monitoring of cutaneous nerve fiber loss during diabetes. Fluorescent fibers in skin sections from the leg of *thy1*-YFP mice stained positive for the neuron-specific protein gene product 9.5 (PGP9.5), indicating that the cutaneous fluorescent fibers are indeed nerve fibers. In diabetic *thy1*-YFP mice, significant small cutaneous nerve fiber loss in the leg was observed at 3 months following the onset of diabetes, but loss of heat-induced pain perception occurred as early as 1 month following the onset of diabetes, indicating that functional impairment of sensory nerves precedes cutaneous nerve fiber loss. Immunostaining of skin sections of mice killed at 6 months following the onset of diabetes showed that parallel to the loss of small fluorescent nerve fibers, there was a significant decrease in fibers stained positive for calcitonin gene–related peptide, substance P, and purinoreceptor subtype in diabetic *thy1*-YFP mice. These mice will be useful for noninvasive monitoring of cutaneous nerve fiber degeneration and loss of heat-induced pain perception during diabetes and for the assessment of efficacy of therapeutic treatment of diabetic neuropathy. *Diabetes* 54:3112–3118, 2005

Neuropathy is one of the most common and debilitating complications in diabetic patients. Peripheral sensory and motor nerve fibers, as well as autonomic nerve fibers, are affected (1). Lesions in the cutaneous sensory fibers may lead to hyperalgesia or hypoalgesia, depending on the stage or the severity of the disease. Hypoalgesia renders patients unaware of the wounds on their lower limbs and, together with impaired wound healing, often causes foot ulceration and gangrene, which may require amputation. There is evidence that the cutaneous nerve might be involved in wound healing as well. Impaired wound healing in diabetic mice was found to be associated with a reduced level of nerve growth factor at the wound site, presumably due to a reduced number of epidermal nerve fibers (2); nerve growth factor has been shown to accelerate wound healing (3,4). In addition to nerve growth factor, the cutaneous nerve may secrete other neurotransmitters and neuromodulators, including catecholamines, acetylcholine, substance P, calcitonin gene–related peptide (CGRP), α-melanocyte–stimulating hormone, and other agents (5). Some of these neuromodulators are known to regulate immune and inflammatory reactions (5). Thus, lesions in the cutaneous nerves contribute to lack of awareness to injuries, impaired wound healing, and impairment in skin immune defense, all key factors contributing to diabetic foot ulceration. Diabetic neuropathy is the leading cause of lower-limb amputation, underscoring the importance of monitoring the integrity of the cutaneous nerves during diabetes and during therapeutic treatment (6).

Different types of cutaneous sensory nerve fibers have been identified. They include the unmyelinated C-fibers, the thinly myelinated A-δ fibers, and the myelinated A-β fibers. C and A-δ fibers are thought to be involved in thermal and pain sensation, whereas A-β fibers are responsible for mechanical sensation. C-fibers are identified by immunostaining with CGRP and substance P (7); however, C, A-δ, and A-β fibers are distinguished only by electron microscopy. In addition to CGRP and substance P (7), immunostaining of purinoreceptor subtype ($P2X_3$) (8) could also be used to identify cutaneous sensory C-fibers, whereas vasoactive intestinal peptide (9) and neuropeptide Y (10,11) staining were used to identify autonomic nerve fibers in skin biopsy samples of diabetic patients. However, most studies used PGP9.5, a neuronal-specific ubiquitin COOH-terminal hydrolase (12), to label all nerve fibers. These studies (9,13–18) indicated that nerve fibers in the epidermis, dermis, and sweat gland were significantly reduced in diabetic patients. Reduction of cutaneous innervation was also observed in animal models. The PGP9.5-positive cutaneous nerve profile, area fraction, and area density were found to be significantly lower in *db/db* compared with db/m mice (2,19). Furthermore, streptozotocin-induced diabetic mice displayed severely reduced cutaneous innervation in the flank and footpad, and intrathecal treatment with glial cell line–derived neurotrophic factor or neurturin was able to stimulate axon regrowth and branching (20). Recently, similar examination of skin

From the [1]Department of Anatomy, The University of Hong Kong, Hong Kong, China; and the [2]Department of Physiology, The University of Hong Kong, Hong Kong, China.

Address correspondence and reprint requests to Dr. Sookja K. Chung, Department of Anatomy, The University of Hong Kong, 8F/S Kadoorie Biological Science Bldg., Pokfulam, Hong Kong, SAR, China. E-mail: skchung@hkucc.hku.hk.

Received for publication 31 March 2005 and accepted in revised form 9 August 2005.

Additional information for this article can be found in an online appendix available at http://diabetes.diabetesjournals.org.

CGRP, calcitonin gene–related peptide; MNCV, motor nerve conduction velocity; $P2X_3$, purinoreceptor subtype; YFP, yellowish-green fluorescent protein.

TABLE 1
Body weight and blood glucose

	1 month		2 months		3 months		6 months	
	Body weight (g)	Blood glucose (mmol/l)	Body weight (g)	Blood glucose (mmol/l)	Body weight (g)	Blood glucose (mmol/l)	Body weight (g)	Blood glucose (mmol/l)
Control	27.0 ± 0.7	7.7 ± 0.2	28.4 ± 0.7	8.0 ± 0.3	29.0 ± 0.5	7.8 ± 0.2	32.1 ± 1.1	7.7 ± 0.2
STZ	19.1 ± 0.9*	31.9 ± 0.7*	21.4 ± 1.2*	31.4 ± 0.5*	22.3 ± 1.6	30.6 ± 1.1*	26.1 ± 1.2†	27.4 ± 1.9*

Data are means ± SE. *$P < 0.001$ by Student's t test; †$P < 0.01$. $n = \sim$15–20 for each group. STZ, streptozotocin-induced diabetic mice.

biopsies from 9-month diabetic mice also showed a reduction in cutaneous axons in the footpad, which was normalized by return of their blood glucose to near euglycemia (21). However, these assessment methods are cumbersome, and such invasive sampling is inappropriate for follow-up studies in live small animals because the small surface areas, like the foot and lower leg, do not allow for repeated sampling. Moreover, the wound created by biopsies may affect the course of the disease. Therefore, a more convenient and noninvasive monitoring of cutaneous nerve degeneration is desirable.

A line of transgenic mice has been generated using the neuron-specific *thy1* promoter to drive the expression of the yellowish-green fluorescence protein (YFP) cDNA (22). All of the sensory/motor neurons in the *thy1*-YFP mice appeared bright yellowish-green when viewed by fluorescence stereomicroscopy. When the hair is removed, we found that cutaneous nerves are also visible as yellowish-green fluorescent fibers when viewed in this manner. In this report, we demonstrate that these *thy1*-YFP mice can be used for noninvasive assessment of small cutaneous nerve fiber degeneration induced by diabetes.

RESEARCH DESIGN AND METHODS

Animal maintenance and genotyping. Male heterozygous *thy1*-YFP (line *thy1*-YFP16) mice backcrossed into C57BL/6 (22) were purchased from The Jackson Laboratory (Bar Harbor, ME). *Thy1*-YFP mice could be quickly distinguished from the nontransgenic counterparts by viewing the fluorescent nerves in the ear/footpad with fluorescence stereomicroscopy (MZFLIII; Leica, Bensheim, Germany) or by PCR (22). Mice were maintained in a 12/12-h light/dark cycle with food and water ad libitum. All studies involving animals followed the guidelines set forth by the committee on the use of live animals in teaching and research from The University of Hong Kong.

Induction of diabetes. Diabetes was induced by a single intraperitoneal injection of streptozotocin (200 mg/kg; Sigma, St. Louis, MO) to 6-week-old mice. Control mice received an equal volume of vehicle (0.1 mol/l citrate buffer, pH 4.5). Tail blood glucose level was determined 3 days later (Glucometer Elite; Pymble, NSW, Bayer, Australia). Mice with ≥20 mmol/l glucose were considered diabetic, and those with ≤8 mmol/l were considered nondiabetic (23). In addition to polyuria, diabetic mice exhibited body weight loss (Table 1).

Quantification of cutaneous small-fiber density. Hair on a defined area of the leg was removed by the application of depilatory cream (Veet, Reckitt Benckiser, Massy, France) 1 day before examination of the cutaneous nerves. Before counting the fibers, mice were anesthetized with hypnorm (Janssen, Oxford, U.K.)/dormicum (Hoffmann-La Roche, Natley, NJ) at a concentration of 0.1 ml/10 g (the resulting mixture of hypnorm/dormicum contained 1.25 mg/ml midazolam, 2.5 mg/ml fluanisone, and 0.079 mg/ml fentanyl). Three squares of 4 × 4 mm each were marked on similar locations on the skin of both legs: midcalf, midthigh, and one in between those two areas. All small fluorescent fibers in each of the squares were counted under the fluorescence stereomicroscope at a magnification of 63×. The density of primary or secondary cutaneous fibers (for definition of primary and secondary fiber, see RESULTS section) in the six aforementioned areas of the legs was expressed as mean number of fibers/100 mm^2 (number of fibers/100 mm^2; $n = \sim$15–20 each for diabetic and nondiabetic groups). The individual counting the nerve fibers was blinded to the experimental groups of the animals. The images of fluorescent fibers in the skin, abdomen, diaphragm, and lower-leg muscle were captured with a Leica DC500 camera attached to the fluorescence stereomicroscope and processed with Leica IM50 software.

Heat-induced pain perception test. Mice were placed on the bottom of a 4-l glass beaker placed in the water bath kept at 55°C. The time it took for the mice to lick their rear paws or jump was recorded. The maximum time for the heat stimulus was 30 s (24).

Motor nerve conduction velocity measurement. Mice were anesthetized with hypnorm/dormicum (0.1 ml/10 g) and kept on the heat pad (FHC, Bowdoinham, ME) to maintain their rectal temperature at 37°C (25). The sciatic nerve was stimulated (5–10 V, 0.05-ms single square-wave pulses) proximally at the level of the sciatic notch and distally at the level of the ankle with a platinum needle electrode (Grass, Quincy, MA). Compound muscle action potentials were recorded from the ipsilateral foot between digits 2 and 3 and amplified, stored, and displayed on a computer (Spike 2; CED, Cambridge, U.K.). An average of ten separate recordings for both proximal and distal latencies and length of sciatic nerve were used for determining motor nerve conduction velocity (MNCV). MNCV was calculated by dividing the distance between stimulation sites over (latency of M wave [notch] − latency of M wave [ankle]).

Histological and immunocytochemical analyses. Sixty-micrometer cryostat sections (from the leg and footpad) were prepared according to the established protocol (22). Images of fluorescent nerve fibers in the cryostat sections were captured under a laser-scanning confocal microscope (LSM410; Carl Zeiss, Jena, Germany) at a magnification of 200×. The lengths of the skin sections were measured by the LSM410 software system. The number of small fluorescent nerve fibers present in the epidermis and upper layer of dermis perpendicular to skin surface was counted (2,16). The density of signals was expressed as linear density, i.e., number of immunoreactive profiles/millimeter (number/mm) (26).

For PGP9.5 immunohistochemistry, rabbit-PGP9.5 antibodies (1:500; Biogenesis) were placed onto 10- or 60-μm skin cryosections and incubated overnight at 4°C. After washing, the tetramethylrhodamine isothiocyanate–conjugated goat anti-rabbit IgG (1:400; Molecular Probe, Eugene, OR) was then added and incubated with the sections for 1 h at room temperature. After another wash, images were obtained with the LSM410 system. Immunostaining with antibodies against rabbit-P2X$_3$ (1:100; Santa Cruz, Santa Cruz, CA), goat-CGRP (1:200; Santa Cruz), and goat–substance P (1:400; Santa Cruz) was performed using a Vectastain Elite ABC kit (Vector, Burlingame, CA) on 10-μm skin paraffin sections. The CGRP-, substance P–, and P2X$_3$-positive nerve fibers were quantitated by counting the total numbers of each nerve type and dividing those numbers by the length of the skin section (26). All counting was performed with images taken with an inverted microscope (IX71; Olympus, Tokyo, Japan), which was connected to a charge-coupled device digital camera RT COLOR Spot (Diagnostic Instruments, Sterling Heights, MI) at a magnification of 40×. Lengths of skin sections were measured using Spot software system. The density of signals was expressed as linear density, i.e., the number of immunoreactive profiles/millimeters (numbers/mm) (26).

Statistical analysis. All data were expressed as means ± SE. Statistical analysis was performed by Student's t test. P values <0.05 were considered to be statistically significant.

RESULTS

The cutaneous yellowish-green fluorescent fibers in the *thy1*-YFP mice are nerve fibers

After removal of a patch of hair from their legs a day earlier, anesthetized *thy1*-YFP mice were placed under a fluorescence stereomicroscope for examination of their cutaneous nerve fibers. Small and large fluorescent fibers were visible when the skin surface was in focus (Fig. 1*A*).

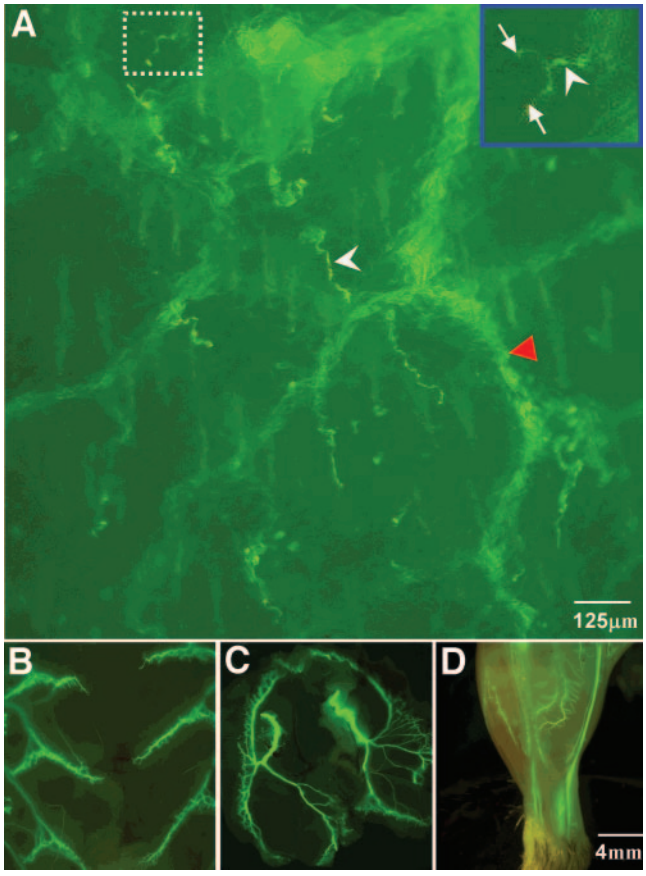

FIG. 1. Photomicrographs showing the cutaneous nerve fibers in the skin surface of the leg (*A*) and the innervation patterns of YFP nerve fibers in abdominal (*B*), diaphragm (*C*), and lower-leg (*D*) muscles. The inset on the upper right-hand corner shows the magnified image of a highlighted small nerve fiber. The white arrowheads point to the primary small fibers, and the white arrows point to the secondary small fibers. The red arrowhead points to the large fiber running in parallel to the skin surface.

However, the larger fluorescent fiber networks running in parallel to the skin surface were more clearly visible only by adjusting the plane of focus. These large fibers were located in the deep layer of dermis. Therefore, we quantitated the small YFP fibers perpendicular to these large fibers, which were mostly located in the epidermis as well as in the upper layer of the dermis (Fig. 1*A*). We were only able to classify them as small fibers, since the magnification used to identify them was too low to determine whether they were myelinated. We defined the small fibers proximal to the large fibers as primary fibers and the small fibers bifurcating from the primary fibers as secondary fibers. We made this distinction because the nerve fibers furthest away from the larger fibers may be more prone to degeneration in chronic diabetes. Although the fluorescent fibers on the footpad were also visible, their image was blurred due to the thickness of the skin, making it difficult to count individual fibers. Besides cutaneous nerves, all other nerve fibers of *thy1*-YFP mice also appeared bright yellowish-green when viewed by fluorescence stereomicroscopy. Examples of fluorescent nerve fibers innervating the abdomen (Fig. 1*B*), diaphragm (Fig. 1*C*), and the sural nerves in the lower leg (Fig. 1*D*) indicate that these nerve fibers could be readily identified without immunostaining for nerve-specific markers.

To confirm that the cutaneous fluorescent fibers are nerve fibers, cryostat sections of the skin on the leg were prepared and stained with antibodies against PGP9.5. Although PGP9.5 is a nerve-specific marker, it could not be used for classifying the specific type of nerve fiber as in the case of YFP nerve fibers. As shown in Fig. 2, the fluorescent fibers also expressed PGP9.5, indicating that they were indeed nerve fibers.

Noninvasive monitoring of cutaneous nerves in diabetic *thy1*-YFP mice

Thy1-YFP mice were made diabetic by streptozotocin injection, and small cutaneous YFP nerve fibers on six defined areas on their legs were counted after 1, 2, 3, and 6 months. As shown in Fig. 3, there was no significant change in the density of cutaneous small fibers after 1 and 2 months of diabetes. However, there was a significant decrease in the density of primary fibers in the 3-month diabetic group compared with the nondiabetic group ($P < 0.001$), and there was a trend toward a decrease in secondary fiber density in this diabetic group compared with the nondiabetic group. After 6 months of diabetes, both primary and secondary fiber densities were significantly decreased ($P < 0.01$ for both primary and secondary fibers).

Reduced perception for heat-induced pain in diabetic mice

Thermal hypoalgesia is one of the characteristics of diabetic small unmyelinated or thinly myelinated fiber neuropathy. Along with monitoring the cutaneous small YFP nerve fibers, hot-plate tests were also conducted after 1, 2, 3, and 6 months of diabetes. The results showed that the delay in response to heat-induced pain was evident at as early as 1 month of diabetes ($P < 0.05$), the first time point in the study (Fig. 4). Hypoalgesia persisted throughout the 6 months of diabetes (2 and 3 months: $P < 0.05$, 6 months: $P < 0.01$).

Verification of cutaneous nerve fiber loss

After 6 months of diabetes, mice were killed, and 60-μm cryostat sections of the skin on the legs and footpads were prepared for examination of fluorescent YFP fibers. Counting of small YFP fibers perpendicular to the skin surface, which were mainly located in the upper part of the dermis and epidermis, showed that there was a significant reduction in the density of small YFP fluorescent fibers (Fig. 5). Immunostaining with PGP9.5 antibodies revealed that all the nerve fibers that stained positive for this antigen also

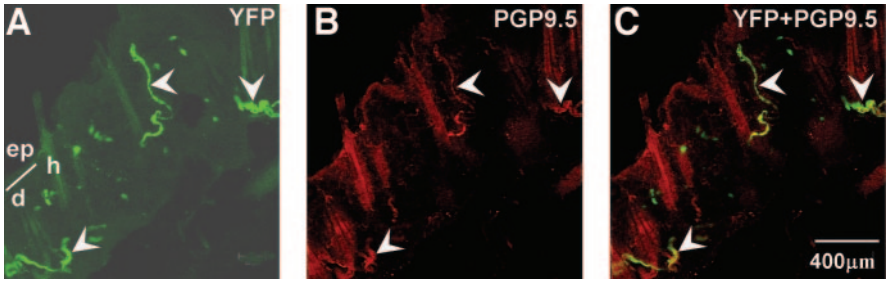

FIG. 2. Photomicrographs showing the YFP cutaneous nerves fibers on 10-μm thick skin sections (green; *A*) were PGP9.5-immunoreactive (red; *B*), and the merged images were yellowish (*C*). The arrowheads indicate the nerve fibers. The boundary between the epidermis and dermis is shown. Note the autofluorescence from the hair shaft. ep, epidermis; d, dermis; h, hair shaft.

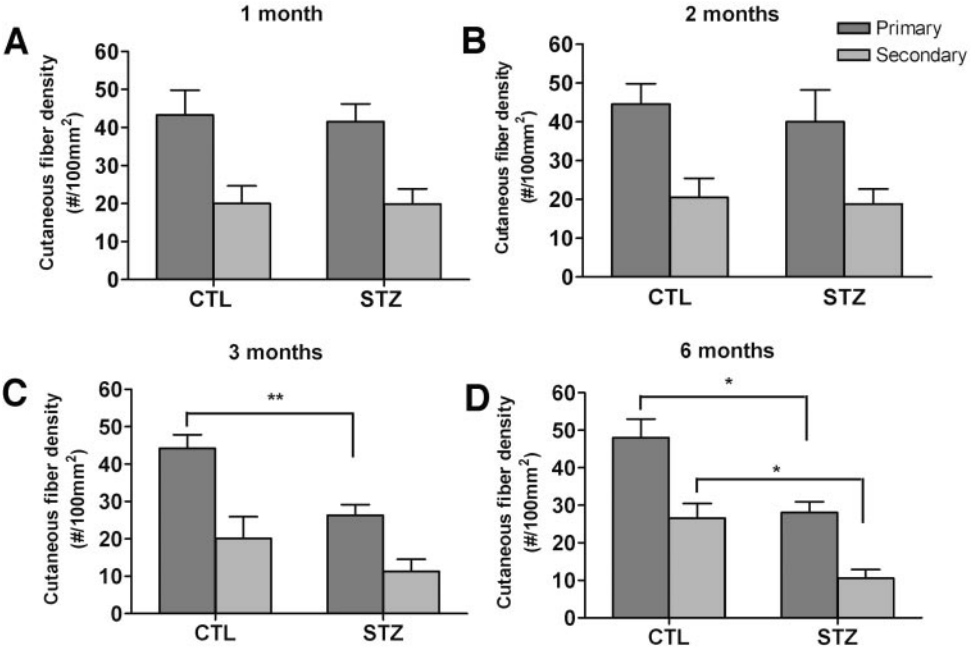

FIG. 3. The histograms showing that primary and secondary cutaneous YFP fiber densities were unchanged after 1 (*A*) and 2 (*B*) months of diabetes. The primary cutaneous fibers were reduced after 3 (*C*) and 6 (*D*) months of diabetes, while the secondary cutaneous fibers were reduced after 6 months of diabetes (*D*). *n* = ~15–20 for both diabetic and nondiabetic groups. CTL, control; STZ, streptozotocin-induced diabetic mice; Primary, primary fibers; Secondary, secondary fibers. **P* < 0.01, ***P* < 0.001 by Student's *t* test.

showed fluorescent yellowish-green color regardless of their sizes (online appendix [available at http://diabetes.diabetesjournals.org]), indicating that the reduction in the number of YFP fluorescent fibers in diabetic mice is not the consequence of inhibition of the expression of the YFP transgene but the result of nerve fiber degeneration.

Since the YFP transgene labeled all sensory and motor neurons, to further determine which subtypes of the cutaneous nerve fibers were lost in the 6-months diabetic mice, paraffin-embedded sections of the skin from the legs of the mice were immunolabeled with antibodies against CGRP (13,20), substance P (13,27), or $P2X_3$ (8). The densities of all three types of nerve fibers in the skin were significantly reduced in the diabetic mice (CGRP: $P < 0.01$, substance P: $P < 0.05$, and $P2X_3$: $P < 0.05$) (Fig. 6).

Reduction of MNCV after 6 months of diabetes

The MNCV, an indicator of functional integrity of peripheral motor neurons, was significantly reduced in the sciatic nerves of the 6-month diabetic mice (Fig. 7*A*, $P < 0.01$). However, linear regression analyses showed that there was no correlation between MNCV deficits and cutaneous nerve fiber reduction (Fig. 7*B* and *C*). Moreover, there was also no correlation between increased heat-induced pain sensation latency and small cutaneous YFP fiber loss after 6 months of diabetes (Fig. 7*D* and *E*).

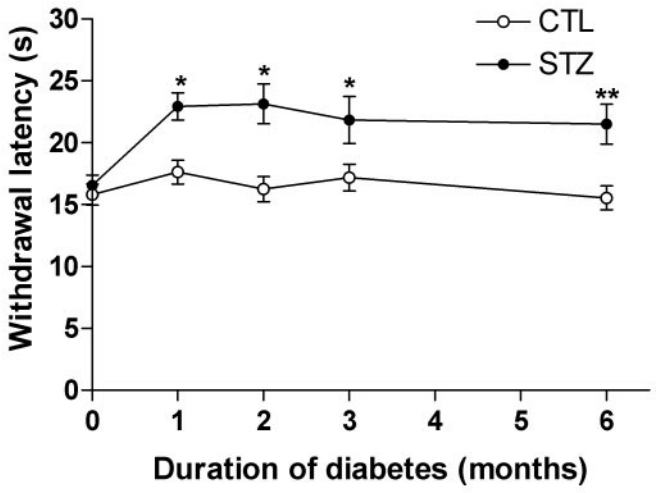

FIG. 4. The histogram showing that the heat-induced pain thresholds (withdrawal latencies) were delayed after 1, 2, 3, and 6 months of diabetes. *n* = ~15–20 for both diabetic and nondiabetic groups. CTL, control; STZ, streptozotocin-induced diabetic mice. **P* < 0.05, ***P* < 0.01 by Student's *t* test.

DISCUSSION

Loss of cutaneous nerve fibers is thought to be partly responsible for the diabetes-induced impairment in the

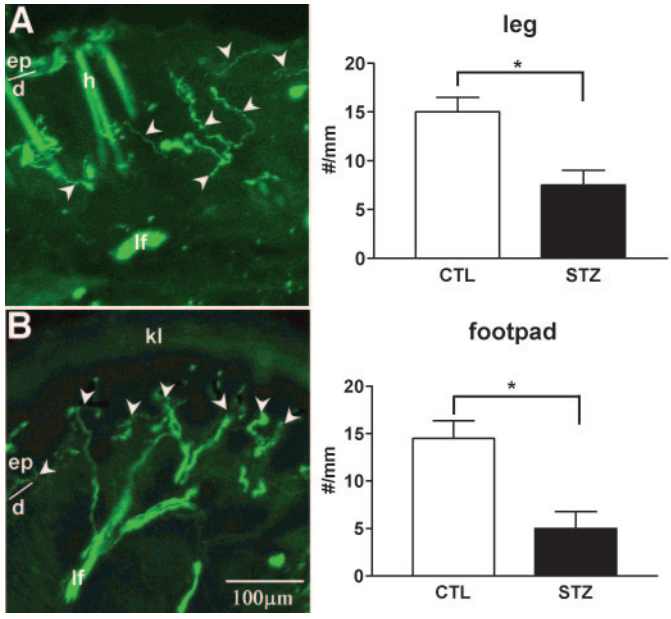

FIG. 5. Photomicrographs showing the cutaneous small YFP fibers in skin biopsy of *thy1*-YFP mice. Cutaneous small fibers were significantly less in the leg (*A*) and footpad (*B*) in 6-months diabetic mice. The arrowheads indicated the nerve fibers. *n* = 5 for both diabetic and nondiabetic groups. The boundary between epidermis and dermis was shown. ep, epidermis; h, hair shaft; d, dermis; kl, thick keratin layer; lf, large fibers. CTL, control; STZ, streptozotocin-induced diabetic mice. **P* < 0.05 by Student's *t* test.

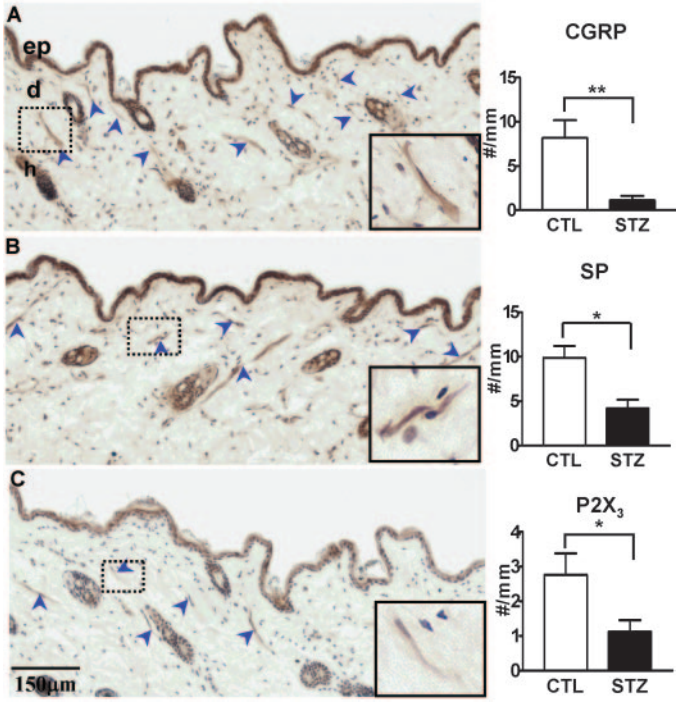

FIG. 6. Photomicrographs showing subpopulation of small nerve fibers in skin biopsy of *thy1*-YFP mice. CGRP (*A*), substance P (*B*), and $P2X_3$ (*C*) immunoreactive nerve fibers were significantly decreased in the skin of 6-months diabetic mice. The arrowheads indicated the nerve fibers. The insets showed the magnified images of the highlighted nerve fibers. $n = 5$ for both diabetic and nondiabetic groups. ep, epidermis, d, dermis, h, hair follicle; CTL, control; STZ, streptozotocin-induced diabetic mice. *$P < 0.05$, ** $P < 0.01$ by Student's t test.

skin's immune defense, wound healing, and pain perception that may lead to foot ulceration and gangrene. The mechanism leading to this diabetic neuropathy is still unclear. We demonstrated that *thy1*-YFP mice provide a convenient noninvasive method of monitoring cutaneous small nerve fiber loss induced by diabetes. We showed that the fluorescent fibers stained positive for the nerve-specific PGP9.5 antigen, confirming that they were indeed nerve fibers. We also showed that the reduction in the number of small cutaneous YFP fluorescent fibers in the 6-months diabetic mice was not due to downregulation of the YFP transgene, as all the PGP9.5 fibers were yellowish-green fluorescent. However, the present noninvasive method of counting the YFP nerve fibers by viewing from the top of the skin only distinguishes small versus large fibers. Electron microscopic analysis of cutaneous axons would be required to classify the types of small YFP fibers. Alternatively, a combined method of immunocytochemical analysis using antibodies specific for the particular subtypes of fibers and quantitation of fibers colocalized with YFP would be useful. However, the drastic reduction in intensity of YFP due to extensive processing of the tissue for immunocytochemical staining would preclude this possibility. The major advantage of using *thy1*-YFP mice for small-fiber loss is that a larger area of the skin can be assessed for changes in the small nerve fibers and that the same skin areas can be monitored over long periods of diabetes. In the future, development of transgenic mice expressing YFP under the control of a C-fiber–specific promoter may allow the noninvasive technique to distinguish the C-type–specific cutaneous nerve fibers from other types of nerve fibers.

In the diabetic mice, loss of cutaneous nerve fibers did

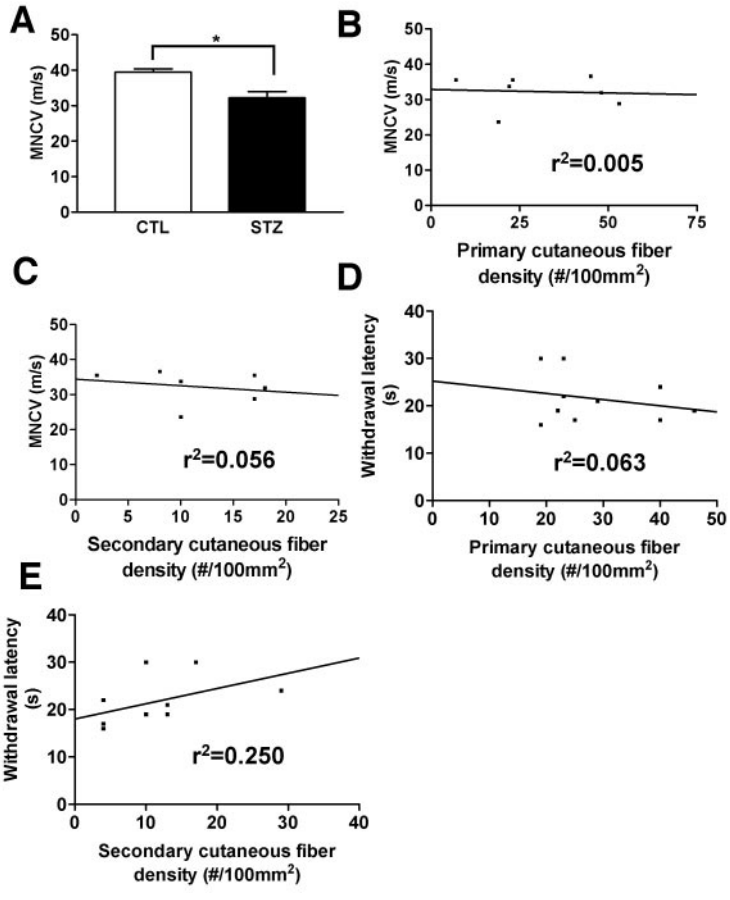

FIG. 7. The histogram showing the correlation of reduction of cutaneous small-fiber density and physiological deficits. MNCV was reduced in 6-months diabetic *thy1*-YFP mice (*A*). There was no correlation between MNCV slowing and decrease of cutaneous fiber density (*B* and *C*). There was also no correlation between the increase of withdrawal latency and the decrease of cutaneous fiber density (*D* and *E*) in 6-months diabetic mice. $n = 9$ for nondiabetic group, $n = 7$ for diabetic group. CTL, control; STZ, streptozotocin-induced diabetic mice. *$P < 0.01$ by Student's t test.

not occur until the 3rd month of diabetes, while functional impairment of the sensory nerve, as indicated by the delayed heat-induced pain response, occurred in the 1st month of diabetes. This finding indicates that functional impairment preceded the loss of small cutaneous YFP nerve fibers, although we could not be certain these YFP fibers are C-fibers. Interestingly, the secondary fibers, which were distal to the main fibers, did not preferentially degenerate before the primary fibers. This suggests that the secondary fibers and the primary fibers, from which they bifurcated, degenerated at the same time. Immunohistochemical analyses revealed that nerve fibers immunoreactive to CGRP, substance P, and $P2X_3$ were all reduced in the skin of the mice that were diabetic for 6 months. The parallel loss of these small sensory fibers and YFP fluorescent fibers further confirmed that the reduction in the number of fluorescent fibers in diabetic mice was due to fiber loss rather than inhibition of expression of the YFP transgene. The CGRP and substance P are markers for sensory fibers involved in nociception and neurovascular dilatory response (9,28,29). The decreased number of these nerve fibers may lead to reduced blood flow to the skin, thereby further exacerbating the degeneration of these nerves. The $P2X_3$-expressing nerves are involved in the pain processing pathway (30). Lacking $P2X_3$-positve sensory nerve fibers may lead to hypoalgesia.

Linear regression analyses showed that reduction of MNCV did not correlate with cutaneous nerve fiber loss. This is consistent with previous observations (13,16) that functional changes, including reduction in MNCV in diabetics, did not correlate with cutaneous fiber changes, confirming that small-fiber deficit does not necessarily reflect lesion in the large fibers.

The YFP transgene is expressed in all sensory and motor neurons in *thy1*-YFP mice, and, as shown in our figures, both small and large nerve fibers are YFP fluorescent. Whereas only the small YFP fibers in the epidermis and upper part of dermis were quantitated in the present study, it is not possible to identify them as C-type fibers. Such a limitation may explain why there is no close correlation between the delayed heat-induced pain response with the reduction of small cutaneous YFP fiber density. In addition, using these mice to monitor cutaneous nerve fiber loss cannot reveal if there is a differential rate of degeneration among different types of nerves. However, the advantage of this noninvasive monitoring of cutaneous nerves is that the fate of individual nerve fibers during the course of diabetes can be followed. There is evidence that regeneration, as well as degeneration, of nerves occurs during diabetes (31,32). Sampling the population of nerve fibers as we have done here only shows the net effect of these two processes. Further studies monitoring a large number of individual small nerve fibers may determine the timing of degeneration. It would also be interesting to determine whether the primary and secondary fibers degenerate at the same time and if the new fibers sprout from the same locations as that of the degenerated fibers. With appropriate markings on the skin, the structure of individual axons can be examined repeatedly over a period of time. The changing structure of the nerve fibers can be recorded by confocal microscope with three-dimensional reconstruction software. Our study demonstrates that *thy1*-YFP mice will be a useful animal model for convenient noninvasive monitoring of cutaneous nerve fiber degeneration during diabetes and that they can also be used to assess the efficacy of drugs for the treatment of diabetic neuropathy. Since all the neurons in these mice are clearly visible with fluorescence stereomicroscopy without the need for immunohistochemical identification, this approach provides a convenient model to study diabetes-induced nerve fiber loss in other tissues.

ACKNOWLEDGMENTS

This project was funded by the Hong Kong Research Grant Council (HKU 7313/04M to S.K.C.).

We thank Prof. Rochelle Cohen for critical reading of the manuscript.

REFERENCES

1. Vinik AI, Park TS, Stansberry KB, Pittenger GL: Diabetic neuropathies. *Diabetologia* 43:957–973, 2000
2. Gibran NS, Jang YC, Isik FF, Greenhalgh DG, Muffley LA, Underwood RA, Usui ML, Larsen J, Smith DG, Bunnett N, Ansel JC, Olerud JE: Diminished neuropeptide levels contribute to the impaired cutaneous healing response associated with diabetes mellitus. *J Surg Res* 108:122–128, 2002
3. Matsuda H, Koyama H, Sato H, Sawada J, Itakura A, Tanaka A, Matsumoto M, Konno K, Ushio H, Matsuda K: Role of nerve growth factor in cutaneous wound healing: accelerating effects in normal and healing-impaired diabetic mice. *J Exp Med* 187:297–306, 1998
4. Muangman P, Muffley LA, Anthony JP, Spenny ML, Underwood RA, Olerud JE, Gibran NS: Nerve growth factor accelerates wound healing in diabetic mice. *Wound Repair Regen* 12:44–52, 2004
5. Luger TA: Neuromediators: a crucial component of the skin immune system. *J Dermatol Sci* 30:87–93, 2002
6. Edmonds M, Boulton A, Buckenham T, Every N, Foster A, Freeman D, Gadsby R, Gibby O, Knowles A, Pooke M, Tovey F, Unwin N, Wolfe J: Report of the Diabetic Foot and Amputation Group. *Diabet Med* 13 (Suppl. 4):S27–S42, 1996
7. Gazelius B, Edwall B, Olgart L, Lundberg JM, Hokfelt T, Fischer JA: Vasodilatory effects and coexistence of calcitonin gene-related peptide (CGRP) and substance P in sensory nerves of cat dental pulp. *Acta Physiol Scand* 130:33–40, 1987
8. Chen C, Akopian AN, Sivilotti L, Colquhoun D, Burnstock G, Wood JN: A P2X purinoceptor expressed by a subset of sensory neurons. *Nature* 377:428–431, 1995
9. Levy DM, Karanth SS, Springall DR, Polak JM: Depletion of cutaneous nerves and neuropeptides in diabetes mellitus: an immunocytochemical study. *Diabetologia* 132:427–433, 1989
10. Pernow J, Saria A, Lundberg JM: Mechanisms underlying pre- and postjunctional effects of neuropeptide Y in sympathetic vascular control. *Acta Physiol Scand* 126:239–249, 1986
11. Edvinsson L, Ekman R, Jansen I, Ottosson A, Uddman R: Peptide-containing nerve fibers in human cerebral arteries: immunocytochemistry, radioimmunoassay, and in vitro pharmacology. *Ann Neurol* 21:431–437, 1987
12. Wilkinson KD, Lee KM, Deshpande S, Duerksen-Hughes P, Boss JM, Pohl J: The neuron-specific protein PGP 9.5 is a ubiquitin carboxyl-terminal hydrolase. *Science* 246:670–673, 1989
13. Levy DM, Terenghi G, Gu XH, Abraham RR, Springall DR, Polak JM: Immunohistochemical measurement of nerves and neuropeptides in diabetic skin: relationship to tests of neurological function. *Diabetelogia* 35:889–897, 1992
14. Properzi G, Francavilla S, Poccia G, Aloisi P, Gu XH, Terenghi G, Polak JM: Early increase precedes a depletion of VIP and PGP-9.5 in the skin of insulin-dependent diabetics: correlation between quantitative immunohistochemistry and clinical assessment of peripheral neuropathy. *J Pathol* 169:269–277, 1993
15. Kennedy WR, Wendelschafer-Crabb G, Johnson T: Quantitation of epidermal nerves in diabetic neuropathy. *Neurology* 47:1042–1048, 1996
16. Hirai A, Yasuda H, Joko M, Maeda T, Kikkawa R: Evaluation of diabetic neuropathy through the quantitation of cutaneous nerves. *J Neurol Sci* 172:55–62, 2000
17. Pittenger GL, Ray M, Burcus NI, McNulty P, Basta B, Vinik AI: Intraepidermal nerve fibers are indicators of small-fiber neuropathy in both diabetic and nondiabetic patients. *Diabetes Care* 27:1974–1979, 2004
18. Shun CT, Chang YC, Wu HP, Hsieh SC, Lin WM, Lin YH, Tai TY, Hsieh ST: Skin denervation in type 2 diabetes: correlations with diabetic duration and functional impairments. *Brain* 127:1593–605, 2004
19. Underwood RA, Gibran NS, Muffley LA, Usui ML, Olerud JE: Color subtractive-computer-assisted image analysis for quantification of cutane-

ous nerves in a diabetic mouse model. *J Histochem Cytochem* 49:1285–1291, 2001
20. Christianson JA, Riekhof JT, Wright DE: Restorative effects of neurotrophin treatment on diabetes-induced cutaneous axon loss in mice. *Exp Neurol* 179:188–199, 2003
21. Kennedy JM, Zochodne DW: Experimental diabetic neuropathy with spontaneous recovery: is there irreparable damage? *Diabetes* 54:830–837, 2005
22. Feng G, Mellor RH, Bernstein M, Keller-Peck C, Nguyen QT, Wallace M, Nerbonne JM, Lichtman JW, Sanes JR: Imaging neuronal subsets in transgenic mice expressing multiple spectral variants of GFP. *Neuron* 28:41–51, 2000
23. Song Z, Fu DTW, Chan YS, Leung S, Chung SSM, Chung SK: Transgenic mice overexpressing aldose reductase in Schwann cells show more severe nerve conduction velocity deficit and oxidative stress under hyperglycemic stress. *Mol Cell Neurosci* 23:638–647, 2003
24. Crawley JN: *What' s Wrong With My Mouse? Behavioral Phenotyping of Transgenic and Knockout Mice*. New York, Wiley-Liss, 2000, p. 72–75
25. Yagihashi S, Yamagishi SI, Wada R, Baba M, Hohman TC, Yabe-Nishimura C, Kokai Y: Neuropathy in diabetic mice overexpressing human aldose reductase and effects of aldose reductase inhibitor. *Brain* 124:2448–2458, 2001
26. McArthur JC, Stocks EA, Hauer P, Cornblath DR, Griffin JW: Epidermal nerve fiber density: normative reference range and diagnostic efficiency. *Arch Neurol* 55:1513–1520, 1998
27. Unger JW, Klitzsch T, Pera S, Reiter R: Nerve growth factor (NGF) and diabetic neuropathy in the rat: morphological investigations of the sural nerve, dorsal root ganglion, and spinal cord. *Exp Neurol* 153:23–34, 1998
28. Grant AD, Pinter E, Salmon AM, Brain SD: An examination of neurogenic mechanisms involved in mustard oil-induced inflammation in the mouse. *Eur J Pharmacol* 507:273–280, 2005
29. Vinik AI, Erbas T, Park TS, Stansberry KB, Scanelli JA, Pittenger GL: Dermal neurovascular dysfunction in type 2 diabetes. *Diabetes Care* 24:1468–1475, 2001
30. Cockayne DA, Hamilton SG, Zhu QM, Dunn PM, Zhong Y, Novakovic S, Malmberg AB, Cain G, Berson A, Kassotakis L, Hedley L, Lachnit WG, Burnstock G, McMahon SB, Ford AP: Urinary bladder hyporeflexia and reduced pain-related behaviour in P2X3-deficient mice. *Nature* 407:1011–1015, 2000
31. Behse F, Buchthal F, Carlsen F: Nerve biopsy and conduction studies in diabetic neuropathy. *J Neurol Neurosurg Psychiatry* 40:1072–1082, 1977
32. Archer AG, Watkins PJ, Thomas PK, Sharma AK, Payan J: The natural history of acute painful neuropathy in diabetes mellitus. *J Neurol Neurosurg Psychiatry* 46:491–499, 1983